

## Multiphysics modeling and optimisation of gas flow characteristics in a novel flow metric based gas sensing chamber with integrated heater

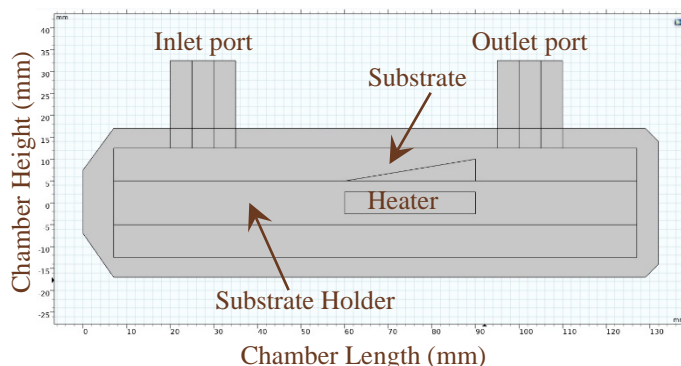
K Govardhan,<sup>1\*</sup> S Muthuraja,<sup>1</sup> A Nirmala Grace<sup>2</sup>

<sup>1</sup>School of Electronics Engineering, Vellore Institute of Technology, Vellore, Tamil Nadu, India. <sup>2</sup>Centre for Nanotechnology Research, Vellore Institute of Technology, Vellore, Tamil Nadu, India.

Submitted on: 27-Oct-2021, Accepted and Published on: 15-Feb-2022

Article

**ABSTRACT** Gas sensors are used very widely in various applications, and it is crucial to test and optimise their performance. A highly reliable gas sensing chamber is vital in proving the credibility of the gas sensor. The paper proposes a flow metric-based gas sensing chamber against the conventional volumetric chamber and presents the gas flow nature in the chamber. The proposed design aims to be portable with an overall length of 132 mm. The inlet port and outlet ports have been optimally placed to reduce the turbulence over the sensing zone. The sensor substrate shape and placement are optimised to attain laminar flow and maximise the gas flow over the sensing surface. Placement of the substrate holder in the flow path of the gas results in a boundary layer, drastically reducing the gas flow over the sensor surface. The substrate angled at 110 and placed at 60 mm from the inlet port exhibited good laminar and close to surface flow over the sensing substrate. This optimised substrate position also exhibited low-velocity flow over the substrate, significantly enhancing the gas sensing performance. The paper also deals with the boundary layer suppression to provide maximal gas flow over the substrate, thereby enhancing the chance of sensing by the gas sensor. A nichrome-based heater is also integrated into the chamber below the substrate holder. The heater integration is necessary since some gas sensors operate at high temperatures for their optimal performance. The heat propagation from the heater onto the substrate holder is also simulated. The voltage applied to the nichrome heater varied from 0 V to 100V, varying from room temperature to 2000 oC. The temperature profile was ideal at 60 V with 850 oC attained over the substrate zone, optimal for most metal oxide gas sensors.



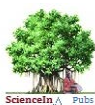
**Keywords:** Gas sensing chamber, Boundary layer, flow in the chamber, Optimisation of the substrate placement

### INTRODUCTION

Gas sensing has become a crucial process in almost every field of science and engineering. It covers the entire spectrum of applications from food processing, medical diagnosis, manufacturing to life comfort. Various materials like metal oxides, semiconducting oxides, etc., and techniques like the thin film, the thick film that has been envisaged, have become commercial products providing very high sensitivity levels even at PPB levels of concentration. Most of these materials and techniques rely on conductive mechanisms to quantify the concentration of gases being sensed. The successful working of

any gas sensor would require a high standard gas sensing chamber, in which the sensor would be tested for its various characteristic behaviours. Unless and until the gas sensing chamber design is reliable, credible, and accurate enough, the characteristics of the sensor cannot be determined to the required standard specifications. These factors emphasise the need for an optimal design of a gas sensing chamber and the study of its characteristic behaviour in terms of gas flow parameters. The design of a gas sensing chamber has to be based on vital performance behaviour characteristics and, at the same time, should provide various salient features when compared to the traditional gas sensing chambers. Many gas sensors perform exceptionally well at optimal temperatures, necessitating that the gas sensing chamber is fitted with integrated heater arrangements. The gas sensing chamber needs to be analysed for its gas flow and thermodynamic responsive behaviours. Gas sensing techniques fall under either chemisorption, chemi-adsorption, or physi-adsorption methods. The best choice to design, build and analyse such a complex multi-domain problem requires a highly sophisticated multiphysics-based computing environment such as COMSOL Multiphysics.

\*Corresponding Author: Dr K Govardhan, Associate Professor, Department of Micro & NanoElectronics, School of Electronics Engineering, Vellore Institute of Technology, Vellore, Tamil Nadu, India.  
Tel: +914162202486  
Email: kgovardhan@vit.ac.in



T.S.Lee<sup>1</sup> has developed a numerical model to investigate fluid flows, laminar flow, and temperature fields through a rectangular cooling chamber. They had considered a pre-heated fluid flow in the chamber. Jaroslav Kralik et al.<sup>2</sup> have developed a mathematical description of flow in one-dimensional large pipe networks, and he has described the flow using flow and pressure dynamics. The laminar flow inside a rectangular channel for its periodicity was studied by Kwankaomeng et al.<sup>3</sup>. This work emphasises the significance of laminar flow inside a channel and various parameters associated with turbulence flow characteristics affecting the relevant effects. Reza Taghavi Z<sup>4</sup> predicted bypass and natural transition in boundary layers by employing Reynolds-averaged Navier-Stokes (RANS) equations on the linear eddy-viscosity turbulence model. The model incorporates different transport equations individually to compute laminar kinetic energy, the turbulent kinetic energy, and the dissipation rate in a flow field.

S.M.Scott<sup>5</sup> has emphasised the requirement for optimal placement of the sensing layer in a chamber. Scott used baffles to optimise flow and orient the sensing chamber to the fluid inflow at optimal angles. The optimisation was carried out based on CFD-based numerical simulations. Damien Biau et al.<sup>6</sup> have investigated numerically and have determined the transition region at which the turbulent flow would transition into laminar flow in a downstream flow. They have also emphasised the fluctuations in the boundary layer and the factors influencing them. Dimitar Marinov et al.<sup>7</sup> have predicted the laminar to turbulent transitions in two-dimensional boundary layers. They have employed near-wall  $k-\epsilon$  turbulence model for simulation of turbulent transport. Mostafa et al.<sup>8</sup> has used Computational Fluid Dynamics to theoretically analyse the pulsating laminar flow in a pipe. They have also studied the behavioural change in the flow due to various control parameters such as Reynolds number, frequency of pulsations, Prandtl number, dimensionless amplitude, and length to diameter ratio.

Benjamin Faigle et al.<sup>9</sup> investigated a multiphysics framework incorporating compositional and non-isothermal two-phase flow inside a porous medium. These concepts were applied to a combined subsurface CO<sub>2</sub> injected in a reservoir, and the flow characteristics were studied. Chu Wang et al.<sup>10</sup> have proposed a numerical framework to model and simulate gas-liquid-solid three-phase flows. They had adopted a non-boundary-fitted approach which effectively avoids frequent mesh-updating procedures. Their work had combined IFEM and CFFT methods to model fluid-solid and gas-liquid interactions accurately. Veremieiev et al.<sup>11</sup> employed Bubnov-Galerkin-based finite element formulation to solve Navier-Stokes and continuity equations to analyse a three-dimensional film over a surface topography. An optimisation study on laminar flow in the channel was studied by Gersborg-Hansen<sup>12</sup> based on the finite element method (FEM) using COMSOL/FEMLAB. They have discussed various optimisation measures taken towards various flow-based problems such as viscous flow, velocity-driven switches, and optimal layout of flow channels in a low to moderate Reynolds number-based flow.

Using computational fluid dynamics software, David Stack et al.<sup>13</sup> have studied the flow characteristics over different structures from a plate to a full cylinder. They have also have investigated the flow behaviour over these structures at low Reynolds number below ten. They have determined the critical aspect ratio between the flow separation and Reynolds number. The boundary layer effect is a concerning factor when dealing with gas sensing chambers. Gas sensing is a highly surface-oriented phenomenon. Fluid flow over a substrate invariably leads to a boundary layer. Various studies have been carried out theoretically and practically to study the impact of the boundary layer on laminar fluid flow characteristics over various geometries<sup>14-22</sup>. S.M.Scott et al.<sup>5</sup> has also done a computational fluid dynamics-based study using the Navier-Stokes equations to determine the fluid's flow characteristics over sensor elements positioned at various facing angles from 0° to 90°. It has been inferred that the sensor response is strongly dependent on the position of the sensor facing the incoming fluid flow. Optimised sensor position was determined to be a negligibly thin sensor element with the sensor placed at 0° to the incoming flow. This idea would be theoretically possible. The sensor element would have a finite thickness and eventually result in a boundary layer when experiencing a flow over it. This requires the sensor element to be positioned at an angle facing the incoming fluid flow to minimise the boundary layer effect. Various flow-related studies based on a multitude of techniques have yielded a complete understanding of laminar flow characteristics, turbulent to laminar flow transition, and vice versa<sup>23-27</sup>.

## COMSOL

COMSOL is a Multiphysics software used to model, simulate, and analyse structures, devices, and systems by subjecting various boundary conditions and parametric loads. The software specialises in analysing Multiphysics-based problems with effective cross-coupling between different parameters<sup>30</sup>. Computational Fluid Dynamics, Single-Phase Flow, Laminar Flow, Turbulent Flow modules, and physics of COMSOL were used to simulate and analyse the model in the software.

## DESIGN OF CHAMBER

### Motivation for the research:

Characteristic and behavioural study of gas sensors is highly critical to sense gas and calibrate the sensor's response in a multi-gas sensing environment. A highly reliable gas sensing chamber is the only option to study the gas sensor's response close to their actual response. Currently employed gas sensing chambers are designed on a volumetric technique as shown in figure 1. In these volumetric based gas sensing chamber, the sensor is placed in an enormous chamber and exposed to a gas or mixture of gases. These gas chambers have a few vital disadvantages. Due to their volumetric nature, these gas chambers would necessitate a large volume of gas samples, on the order of a few litres. Moreover, they work on the gravimetric principle. The gas sensor is placed at the bottom of the chamber, and the exposed gas needs to reach the sensor to react and provide a response.

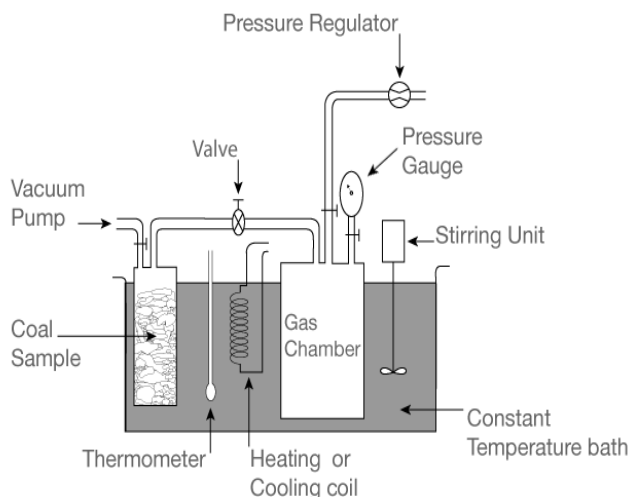


**Figure 1.** Schematic of the Volumetric Chamber Design

The gas sensors would require to be operated at an optimal temperature in the range of a few hundred degrees Celsius to bring about the maximum efficiency of the gas sensor. The heat spread in the chamber also would not be uniform, creating a highly disturbed thermodynamic environment. Elevating or subsiding the temperature in the chamber would take longer time intervals ranging from a few minutes to a few hours. The heat rise and fall gradients would require extensive time intervals of the sensor, resulting in more significant sample analysis time durations. These gas sensing chambers are also mostly gravimetric. The gas sensor is placed at the bottom of the chamber, and the gas must be passed in the chamber until the entire chamber is filled with the required gas. If not, most of the gases would typically settle towards the top of the chamber, and the sensor is not being exposed to the required concentration of measured gas. Gas filling in the chamber and settling in the chamber is also a tedious, time-consuming process. In order to avoid all the cons mentioned above in the traditional gas sensing chamber design, a new flow metric gas chamber design is being proposed and has been analysed for the gas flow characteristics.

#### Gas Sensing Chamber Requirements

A highly efficient gas sensor testing chamber is very vital for reliable testing of gas sensors. This critical requirement is defined based on various parameters. Gas flow characteristics inside the chamber govern the working of the gas sensor testing chamber. A gas chamber would have one or more inlet ports for intake of gases for sensing and at least one outlet port for exhaust gas to be vented out. The gas chamber in cylindrical shape would be ideal for obstruction free-flowing of gas through it. The gas proposed gas sensing chamber was designed with two inlet ports and one outlet port as shown in figure 2. The chamber was designed as a hollow cylinder with an internal diameter of 25 mm and an external diameter of 30 mm with an external length of 132 mm. The chamber was designed to have an active flow length of 120 mm through which the gas flows. Gas flow venting from an inlet port of a smaller diameter into a wider chamber would lead to a turbulent flow. This turbulent flow needs to be transformed into a laminar flow either actively or passively. Unless the flow is

laminar over the substrate, the gas sensing would not be efficient. Various studies and relevant optimisation need to be undertaken to make the flow laminar. Other effects due to the boundary layer need to be suppressed to achieve laminar flow over the substrate.

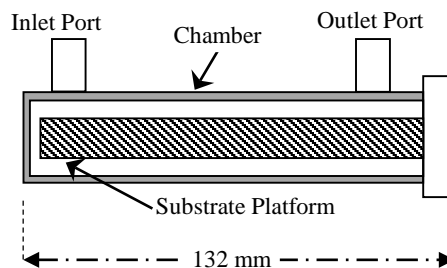


**Figure 2.** Schematic of the Flowmetric Chamber Design

#### Flow Chamber Model:

The flow chamber model was designed and analysed in COMSOL Multiphysics, a FEM-based Multiphysics software. The model was designed with an integrated heater as its vital component. Nichrome wire was used as the heating element. The heater element was encased in stainless steel is made up of stainless steel and a heating element with nichrome wire. The heater rod is cylindrical, with 126.8 mm in length and 10 mm in diameter. The stainless-steel encasing doubles as the substrate holder platform. Again, the substrate holder is a stainless-steel plate assumed to be fixed firmly with the substrate holder platform for both rigid support and effective heat conduction from the heater to the substrate via the substrate holder platform and the substrate holder. The substrate holder is modelled with dimensions of 20 mm in length. This heater rod cum the substrate platform with the substrate holder is modelled as a combined component that can be fitted inside the chamber. The substrate holder needs to be optimised for its lateral positioning on the substrate holder and its angular position with respect to the gas flow in the chamber. The gas inlet is designed to feed the gas into the chamber at right angles to the axis of the flow chamber. The gas exhaust is designed to evacuate the gas at right angles. The chamber is long enough for the flow to be laminar over the substrate.

#### GAS FLOW STUDIES

##### Initial Boundary Conditions

The study of gas flow characteristics and their optimisation should be based on various boundary conditions, initial conditions, and physics-based characteristic equations. The behaviour of the gas flow in the chamber depends on multiple factors, including material properties like the density of the gas, its dynamic viscosity, design parameters like length of the flow and velocity of the flow. The initial conditions to be defined are based on a stable state with no flow initiated in the chamber. The problem is solved using Navier-Stokes equations with Single-Phase Flow interfaces applied in the compressible formulation of the continuity equation given below<sup>30</sup>.

The foremost initial boundary condition to be assumed would be that no fluid flow was present in the chamber before analysis.

$$\frac{\partial \rho}{\partial t} + \nabla \cdot (\rho u) = 0; \quad \rightarrow(1)$$

The momentum equation of the fluid flow must be applied along with the boundary condition as mentioned in the above equation.

$$\rho(u \cdot \nabla)u = \nabla \cdot \left[ -pI + \mu(\nabla u + (\nabla u)^T) - \frac{2}{3}\mu(\nabla \cdot u)I \right] + F \quad \rightarrow(2)$$

The flow characteristics are dependent on various parameters given in both the above equations.

Boundary conditions at the inlet port are considered with  $p = P_0$ , where inlet flow pressure is defined by the variable  $P_0$ <sup>[31]</sup>.

$$\left[ \mu(\nabla u + (\nabla u)^T) - \frac{2}{3}\mu(\nabla \cdot u)I \right] n = 0 \quad \rightarrow(3)$$

where  $\rho$  denotes density (kg/m<sup>3</sup>),  $u$  denotes the flow velocity field,  $\mu$  denotes dynamic viscosity (Pa·s),  $p$  denotes pressure (Pa),  $I$  represent a unit diagonal matrix, and  $F$  denotes the volume force acting on the liquid.

**Laminar flow over the substrate**

The working of a gas sensing chamber relies on the flow characteristics of the gas flowing in the chamber. The gas flow over the sensing layer must be laminar rather than turbulent. There is a higher possibility of turbulence when fluid enters a chamber with different pressure gradients with a specific flow rate. The gas requires to be allowed to flow over a certain distance to change into a laminar flow. This transition zone needs to be positioned well ahead of the substrate holder. The substrate holder region should lie in the laminar region following the turbulent to the laminar transition region. The sensing layer should be ideally placed in this laminar flow region to attain maximum sensitivity.

The flow rate at the inlet is approximately 0.1 mm/s. The Reynolds number, which is essential for characterising the flow, is given by:

$$Re = (\rho U D) / \mu \quad \rightarrow(4)$$

where  $\rho$  is the fluid density (in kg/m<sup>3</sup>),  $U$  is a characteristic velocity of the flow (in m/s),  $\mu$  is the fluid viscosity (in Pa·s), and  $D$  is the average diameter of the flow channel, which in this case is the cylindrical diameter<sup>28-30</sup>.

The laminar flow in the pipe is defined by Navier-Stokes law given as

$$\rho U \cdot \nabla U = -\nabla P + \nabla \cdot T + \rho G \quad \rightarrow(5)$$

where  $P$  is the gauge pressure,  $T$  is the viscous stress tensor, and  $G$  is the acceleration due to gravity<sup>11</sup>.

The volume force node specifies the volume force  $F$  on the right-hand side of the momentum equation.

$$\rho \frac{\partial u}{\partial t} + \rho(u \cdot \nabla)u = \nabla \cdot \left[ -pI + \mu(\nabla u + (\nabla u)^T) - \frac{2}{3}\mu(\nabla \cdot u)I \right] + F$$

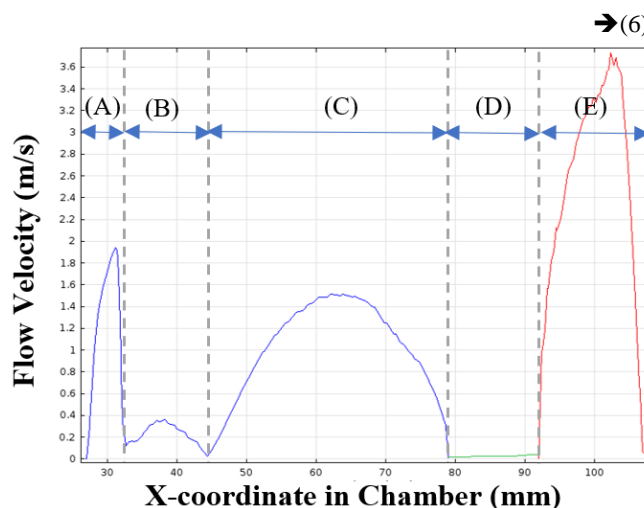


Figure 3. Velocity Profile of Gas flow in the chamber

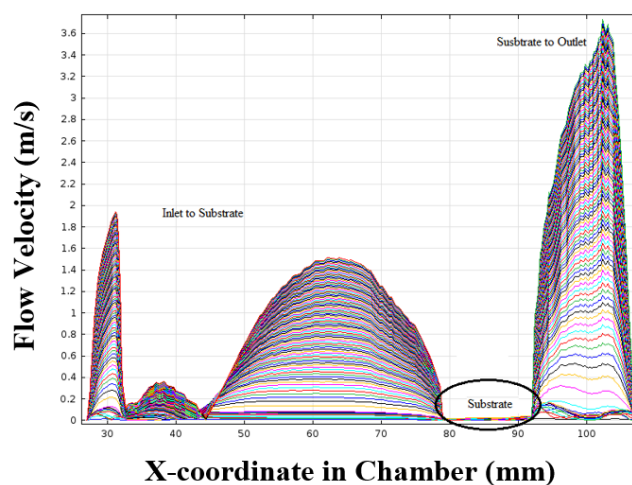


Figure 4. Velocity Profile of Gas flow in the chamber over Sweep in Inlet Pressure

The velocity profile map of the entire chamber as presented in figure 3 indicates various zones of turbulence and laminar flow. The gas flow enters the chamber through an inlet port. The gas flows higher through the inlet port due to its narrow dimensions, as indicated in 'A' portion. The Reynolds number of the flow was calculated to be as 2374.3057 in this chamber zone. The gas release from a narrow inlet port to wide chamber results in turbulence observed in zone 'B'. The Reynold number of the flow got reduced to 1826.2889 due to the expansion of the gas to a higher volume chamber. The gas flow turns into a laminar flow from turbulent nature depending upon the distance of flow inside the chamber, which is showcased in zone 'C'. The flow gets highly laminar near the substrate holder and continues to flow

over the substrate in a laminar mode. The substrate holder is optimally positioned at the laminar flow zone of the gas flow, as seen in zone 'D'. Due to the very low gas velocity, the laminar flow region would have a meagre Reynolds number ranging between 14.6111 and 41.39815. The flow zone 'D' showcases that the velocity is just one-hundredth of the maximum flow velocity value inside the chamber. The flow volume shrinks near the chamber's exit vent, zone 'E', resulting in a high-velocity flow and turbulence. This flow gets subdued as the flow exits through the exhaust port. The Reynolds number of the flow in this zone reaches a maximum of 4505.93. The simulation at various flow rates positively indicates that the flow trend is similar for a wide range of flow rates and inlet pressure parametric variations. This concludes that the substrate holder placement is optimal for the given chamber design.

When many volume force nodes are added to the same domain, the sum of all individual contributions is added to the momentum equations<sup>30</sup>. The overlapped velocity profile of the gas sensing chamber showcased in figure 4 illustrates that the gas flow through the chamber exhibits a similar behaviour in their respective zones. This analysis is essential when analysing a chamber with multiple inlet ports.

#### Boundary-Layer Effect on the Velocity Profile over the substrate

When gas flows over any obstacle, a boundary layer is established depending on the velocity of the flow and the angle at which the gas strikes the substrate. The same can be viewed from figure 5 near the edge facing the inlet flow. The boundary layer thickness increases in direct proportion to both parameters.

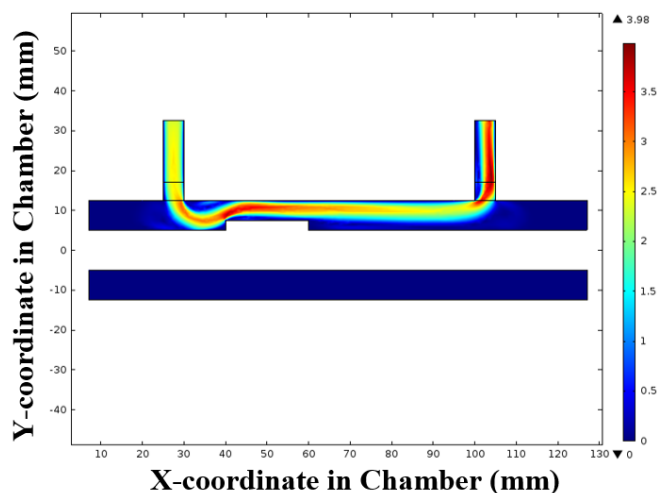


**Figure 5.** Velocity Profile of Gas flow in the chamber with substrate at 40 mm

The position of the substrate becomes very critical in suppressing the boundary layer effect. The boundary layer thickness depends on the angle at which the gas flows past substrate zone, the velocity of the gas flow, the substrate's thickness, and its position relative to the gas entry into the chamber. The boundary layer is created when the gas flow

experiences a sudden vertical obstacle in its flow path. The boundary layer thickness would increase with the gas flow velocity. This indicates that the substrate must be placed in a zone with a minimum gas flow velocity over it. When the substrate is directly below the gas inlet, the velocity of the flow acting on the substrate is very high and with a turbulent influence. When the substrate is placed too far off from the inlet port but closer to the outlet port, the flow becomes turbulent near the outlet port. The optimal position would be in the laminar flow zone before the transition point at which the flow turns back from laminar to turbulent.

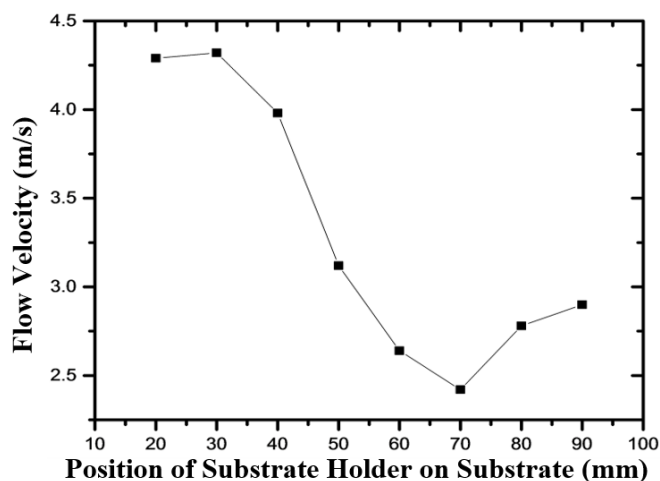


**Figure 6.** Velocity Profile of Gas flow over the Substrate at various positions in the chamber

The model was analysed for the gas flow velocity profile by placing the substrate at different distances from the flow inlet. The flow velocity was observed to be minimum at 70 mm as indicated in figure 6.

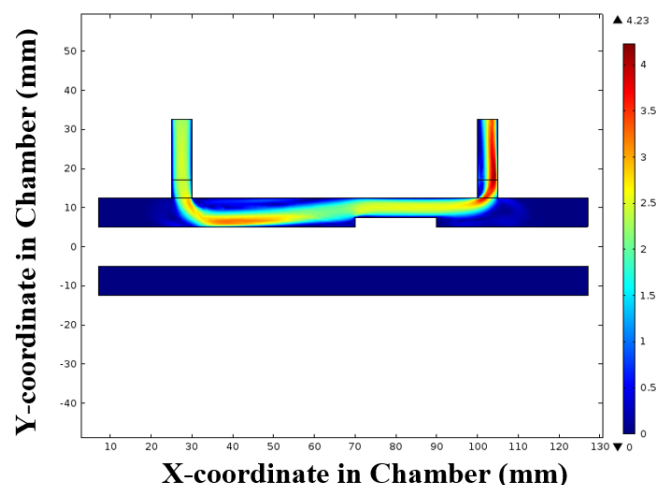


**Figure 7.** Optimal Velocity Profile of Gas flow over the Substrate at 70 mm in the chamber

The velocity was observed to be minimal when the substrate was placed at 70 mm in the chamber. The results indicate that the boundary layer is significantly small near the substrate top surface at this optimal position of the substrate as shown in figure

7. The flow velocity is on the higher side at other substrate positions. It is evident from the previous results that any obstacle placed in the gas flow path would result in a boundary layer. Higher the boundary layer, less gas will flow near the substrate, thus resulting in ineffective sensing as fewer reactants are available for the active sensing surface.

#### Boundary-Layer Effect due to Thickness of the Substrate on the Velocity Profile over the Substrate

The thickness of the boundary layer depends on the surface's height facing the gas flow and would result in a thicker boundary layer. The gas flow over a sudden obstruction in the flow path forms a boundary layer. A vortex in the flow typically characterises the leading edge of the boundary layer, and this vortex, along with the flow velocity, determines the boundary layer thickness. The boundary layer and the associated vortex should be maintained to achieve a good sensing mechanism at the minimum possible level. The substrate holder and the substrate mounting would be the prime causes for the boundary layer. The flow would be highly laminar throughout the maximum part of the flow in the absence of the substrate holder and the substrate in the chamber as per the simulation results presented in figure 8.

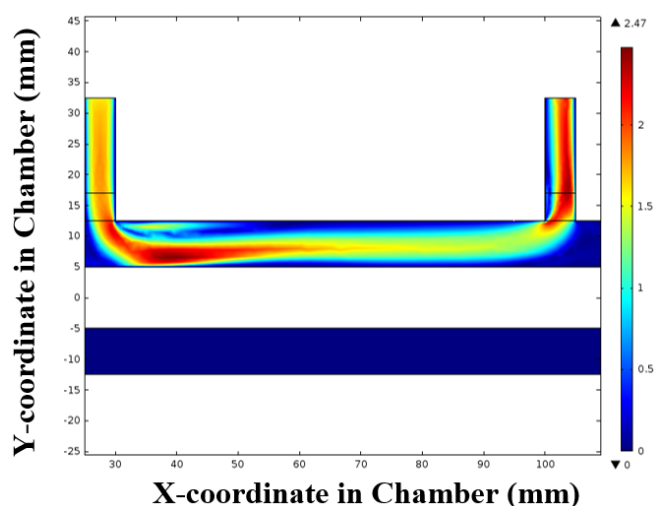


Figure 8. Absence of Boundary Layer with no Substrate

However, there would be a slight upward flow movement observed in this chamber caused by the inlet flow directed toward the bottom wall of the chamber which can be clearly observed in figure 9 towards the trailing edge of the flow. This upward flow depends on the inlet flow velocity, outflow port position, the outflow port exhaust pressure, etc. The Boundary layer effect can be prominently observed with the introduction of the substrate. The height of the substrate surface facing the gas flow dictates the boundary layer over the substrate.

#### Suppression of Boundary Layer Effect by Optimising the Flow Facing Angle of the Substrate

The flow through the chamber is characterised by various zones of flow nature, including zones of turbulent and laminar flow. The flow near the inlet and outlet ports exhibits a turbulence flow nature. The inlet flows striking the substrate base platform would result in a small vortex around 60mm to 70 mm in the chamber for various pressure ranges.

The optimal position of the substrate is preferred to be between 70 mm and 90 mm due to the laminar flow of the gas in this range. But even in this range, the boundary layer could not be eliminated. The placement of the substrate would result in turbulence. To suppress the boundary layer, if not eradicate it, an angled substrate placement with respect to the gas flow would be preferred. The angled substrate would assist the gas is flowing in a more laminar nature over the substrate. The optimised angle of the substrate would reduce the boundary layer to a very low thickness. The flow characteristics over the substrate are more laminar with a very low-velocity magnitude, leading to an excellent sensing efficiency. Lund et al.<sup>32</sup> have achieved gradient-based shape optimisation based on fluid-structure interaction. They have employed RANS with the Baldwin-Lomax turbulence model to design the optimised gradient shape of the obstacle in the flow to attain laminar flow over the substrate.

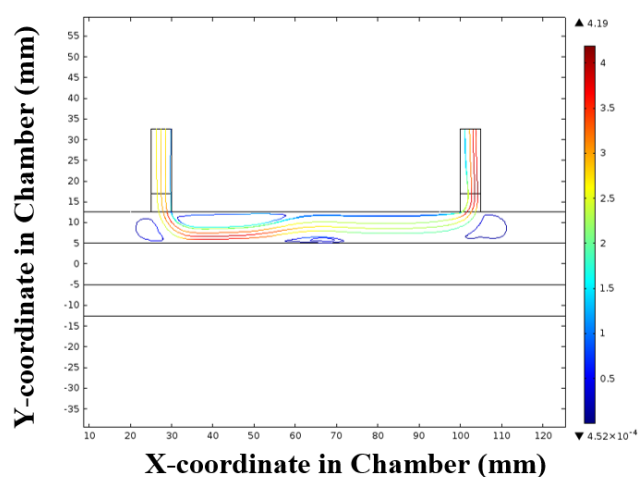


Figure 9. Velocity Profile of Gas flow in the chamber without the substrate

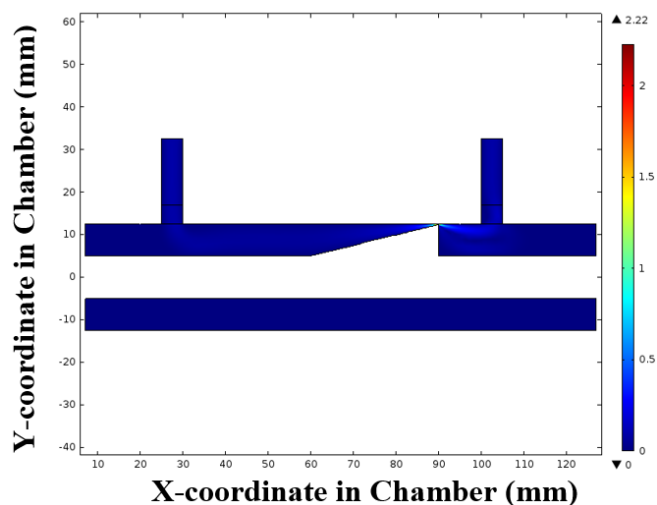
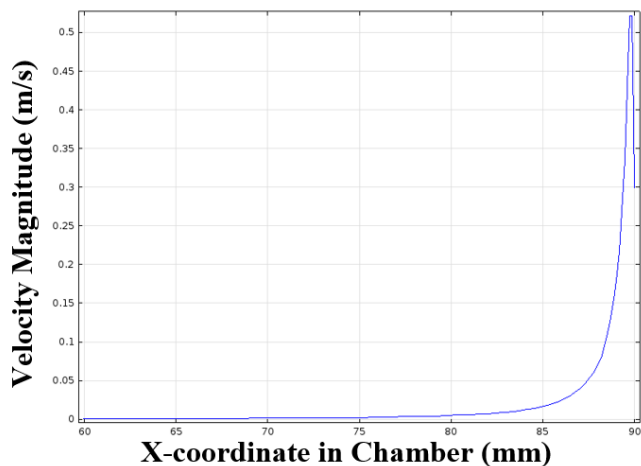


Figure 10. Velocity Profile of Gas flow over the substrate angled at 22 degrees

The angle of the substrate can be varied between  $0^\circ$  to  $21^\circ$  in the chamber, beyond which the flow would be completely cut off over the substrate. Even in the absence of the substrate, the flow is turbulent before the 70 mm position and after the 90 mm

position. This turbulence is primarily caused by the inlet flow directed towards the bottom wall of the chamber. The chamber is designed to be flow metric in nature tends to have thinner diameters and longer horizontal flow paths. The flow was not allowed to flow over substantially longer distances vertically to stabilise. The turbulent nature of the flow is observed before the 70 mm position due to the inlet flow bouncing back from the substrate platform and depending on the flow rate or velocity of the inlet flow. A similar turbulence effect is observed after the 90 mm position due to the flow towards the thin exhaust outlet port. This turbulence is dictated by the exhaust port pressure and thickness of the exhaust port. When the substrate is angled to the maximum of 22°, the flow is almost completely cut off, resulting in a near-zero velocity of flow over the substrate and high turbulence at the peak of the substrate at 90 mm as presented in figure 10 and 11.

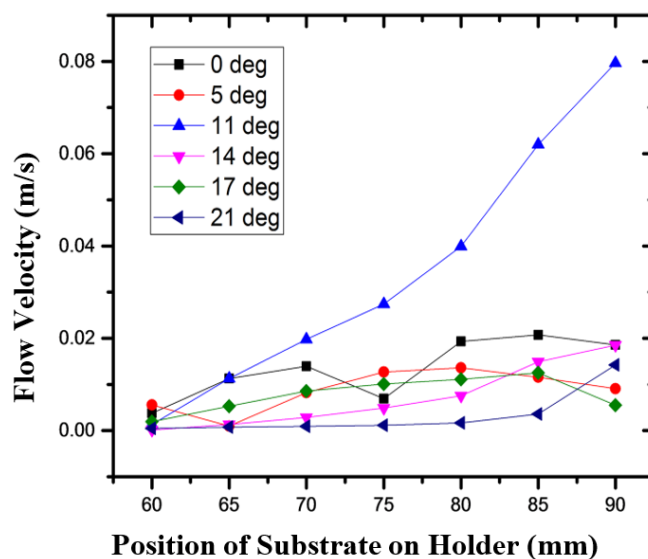
At smaller angles, the flow has an inherent boundary layer, and at larger angles, the flow is minimal over the substrate. The velocity increases exponentially towards the trailing edge of the substrate.



**Figure 11.** Velocity Profile of Gas flow over the substrate angled at 22 degrees

**Figure 12.** Velocity Profile of Gas flow over the substrate angled at various angular position of substrate

The angle needs to be optimised between the two extremes of 0° and 22°. The simulation results, shown in figure 12 provides the data on velocity profile over the substrate placed between 60 and 90 mm, but with various angles like 0°, 5°, 11°, 14°, 17° and 21°. The flow was cut-off at 22°. The flow velocity was dependent on the substrate angle and clearly shows that turbulence prevails at lower and higher substrate angles with reference to the gas flow path. The constant flow rate over the substrate, being the characteristic nature required for good gas sensing, is observed when the substrate is positioned at an optimal angle of 11°, as can be observed from figure 13.



The gas flow velocity increases over the substrate from the leading edge to the trailing edge. The flow is optimised to be laminar without any turbulence over the substrate when the substrate was angled at 11°. The optimal position and the angle of the substrate had suppressed the boundary layer effect to a minimal level over the substrate.

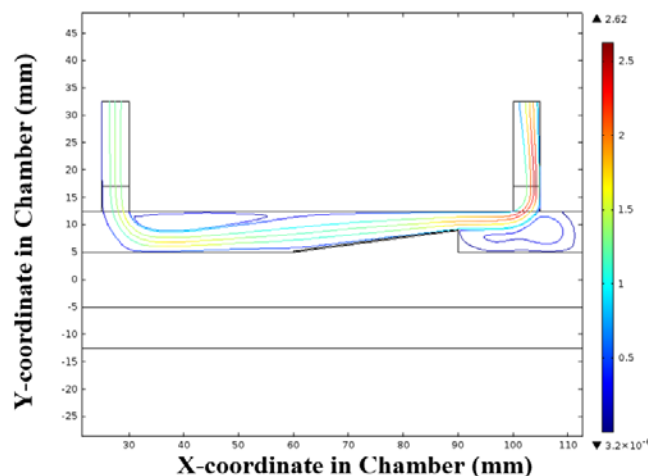


**Figure 13.** Optimized Laminar Flow over the Substrate

### HEAT PROPAGATION FROM HEATER TO THE GAS FLOW IN THE CHAMBER

The gas chamber was designed with an integrated heating system based on a nichrome heater. The nichrome heater material is encapsulated in a stainless-steel casing which doubles as the substrate holder. The stainless-steel casing also acts as an excellent heat transfer medium that conducts heat from the heater and transfers it to the substrate holder. The gas flowing in the chamber gets heated while it comes in contact with the stainless substrate holder. The heat transfer equations with the relevant boundary conditions are given by,

$$\nabla \cdot (-k \nabla T) = 0 \quad \rightarrow (7)$$

and

$$-n \cdot (-k \nabla T) = q_0 + h(T_{\text{inf}} - T) - \nabla_t \cdot (-d_s k_s \nabla_t T) \quad \rightarrow (8)$$

where  $n$  is the normal vector of the boundary,  $k$  is the thermal conductivity (in  $\text{W}/(\text{m}\cdot\text{K})$ ),  $h$  is the heat transfer film coefficient (in  $\text{W}/(\text{m}^2\cdot\text{K})$ ), and  $T_{\text{inf}}$  is the temperature (in  $\text{K}$ ) of the surrounding medium. The additional flux given by the thin conducting layer is included in the equation, and the constant  $k_s$  is the thermal conductivity in the layer (in  $\text{W}/(\text{m}\cdot\text{K})$ ).

The heat transfer from the substrate holder to the gas can be modeled as a heat transfer onto a thin heat-conducting layer of the gas that comes in contact with the heater or the substrate. The inward heat flux  $q_0$  is equal to  $q_{\text{prod}}$ , heat flux produced due to the influence of the electric potential applied to the heater. The heat power per unit area (in  $\text{W}/\text{m}^2$ ) produced in the thin layer is given by

$$q_0 = q_{\text{prod}} = dQ_{DC} \quad \rightarrow (9)$$

$$\rho C_p \frac{\partial T}{\partial t} - \nabla \cdot (k \nabla T) = Q_e \quad \rightarrow (10)$$

where  $\rho$  is density, heat,  $C_p$  is heat capacity,  $k$  is thermal conductivity, and  $Q_e$  is the heat flux derived from the electromagnetic heat source. The equation is based on Fourier's law of heat conduction. The heat source depends on the  $E$ , electric field strength (in  $\text{V}/\text{m}$ ), and  $J$  is the current density (in  $\text{A}/\text{m}^2$ )

$$Q_e = J \cdot E \quad \rightarrow (11)$$

The heat produced by the electromagnetic heat source is controlled in terms of the voltage applied to the nichrome heater. The heat transfer from the heater onto the steel encasing needs to be maximum around the substrate holder, hence the thin film gas sensor. The heater is placed below the substrate holder to achieve this. The heat from the heater also gets transferred to the gas in the chamber. This helps in attaining pre-heating of the gas in the chamber before coming in contact with the sensing layer. It prevents partial cooling of the sensing layer due to comparatively cooler gas flow. The heat transfer pattern in the chamber can be visualised below in figure 14.

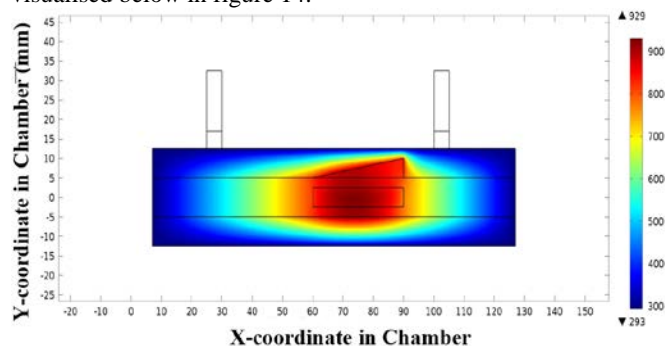


**Figure 14.** Surface Temperature Profile in the Chamber at Heater Potential of 60 V

The heater is excited through a range of voltages, generating heat transferred to the substrate holder. The heat transferred to the substrate holder needs to be uniform all along its dimensions for a wide range of temperatures. The temperature over the substrate is uniform at lower temperatures (up to 1000 K), beyond which the temperature slightly fluctuates due to the gas flowing over the surface. The temperature profiles for heater potential varying from 0 to 100 V are shown below in figure 15.

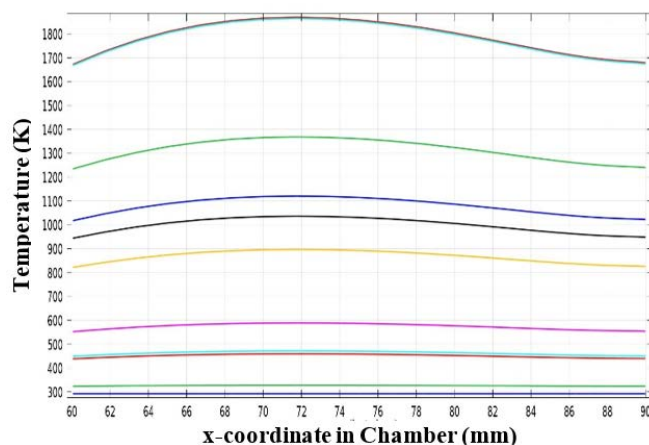


**Figure 15.** Temperature Profile over the Substrate for various Heater Potentials

## CONCLUSION

A flow metric-based gas sensing chamber is modelled simulated for its characteristic performance. The gas flow characteristics in the chamber were simulated. The turbulence caused by the flow into the chamber from a narrow inlet port and the exhaust through a narrow outlet port was studied. Substrate placement in between these turbulence zones was optimised for various parameters. The main optimisation is based on achieving laminar flow over the substrate. The flow over the substrate is affected by boundary layer effects if the substrate holder is placed very near the inlet. The flow over the substrate is turbulent when placed near the outlet owing to the exhaust port angle. The optimal placement was decided based on suppression of boundary effect and achieving laminar flow over the substrate. The optimal placement was between 60 mm and 90 mm in the substrate.

Moreover, an enhanced laminar flow with a low, non-zero gas flow velocity was achieved by placing the substrate at the desired angle of 11 degrees facing the inlet gas flow through the chamber. The nichrome-based heater integrated into the chamber adds functionality to model temperature-based effects. The heat transfer from the heater onto the substrate holder and then to the gas flow is analysed and visualised in the study. The design can be further enhanced by optimising the chamber's gas inlet and outlet port placements. The number of inlet ports can be increased to handle more than one gas.

## REFERENCES

1. T.S.Lee. Laminar fluid and heat flow through an opened rectangular cooling chamber, *Int. J. Heat and Fluid Flow*, **1991**, 12, 3.
2. J. Kralik, P. Stiegler, Z. Vostry, J. Zavorka. Modeling the dynamics of flow in gas pipelines, *IEEE Transactions on Systems, Man and Cybernetics*, **1984**, 14, 4, 586-596.
3. S. Kwankaomeng, W. Jedsadaratanachai, P. Promvongse, Laminar periodic flow and heat transfer in square channel with 30° inclined baffles, *Proceedings of the International Conference on Energy and Sustainable Development: Issues and Strategies (ESD)*, **2010**, 1-7.
4. Reza Taghavi Z., Mahmood Salary, Amir Kolaei, Prediction of boundary layer transition based on modeling of laminar fluctuations using RANS approach, *Chinese Journal of Aeronautics*, **2009**, 22, 113-120.
5. S. M. Scott, D. James, Z. Ali, W. T. O'Hare. Optimising of the sensing chamber of an array of a volatile detection system-fluid dynamic simulation, *Journal of Thermal Analysis and Calorimetry*, **2004**, 76, 693-708.
6. D. Biau, D. Arnal, O. Vermeersch, Transition prediction model for boundary layers subjected to free-stream turbulence, *Aerospace Science and Technology*, **2007**, 11, 370-375.
7. D. Marinov, Z. Zapryanov, Numerical modelling of laminar-turbulent transition in the boundary layers under the influence of low free-stream turbulence intensities, *Computer Methods in Applied Mechanics and Engineering*, **1993**, 110, 263-273.
8. H. M. Mostafa, K. K., Abd-Elsalam, A. M., Torki, Theoretical study of laminar pulsating flow in a pipe, *Thermal Issues in Emerging Technologies*, **2007**, 219-224.
9. B. Faigle, M.A. Elfeel, R. Helmig, B. Becker, B. Flemisch, S. Geiger, Multi-physics modeling of non-isothermal compositional flow on adaptive grids, *Computer Methods in Applied Mechanics and Engineering*, **2015**, 292, 16-34.
10. C. Wang, L.T. Zhang, Numerical modeling of gas-liquid-solid interactions: Gas-liquid free surfaces interacting with deformable solids, *Computer Methods in Applied Mechanics and Engineering*, **2015**, 286, 123-146.
11. S. Veremieiev, H.M.Thompson, P.H.Gaskell, Free-surface film flow over topography: Full three-dimensional finite element solutions, *Computers and Fluids*, **2015**, 12, 66-82.
12. Gersborg-Hansen, O. Sigmund, R.B. Haber, Topology optimisation of channel flow problems, *Structural and Multidisciplinary Optimisation*, **2005**, 30, 181-192
13. D. Stack, H.R. Bravo, Flow separation behind ellipses at Reynolds numbers less than 10, *Applied Mathematical Modelling*, **2009**, 33, 1633-1643.
14. T.G. Myers, An approximate solution method for boundary layer flow of a power law fluid over a flat plate, *International Journal of Heat and Mass Transfer*, **2010**, 53, 2337-2346.
15. X. Gao, J. Hu, Numerical Simulation to the Effect of Rotation on Blade Boundary Layer of Horizontal Axial Wind Turbine, *2010 World Non-Grid-Connected Wind Power and Energy Conference (WNWEC)*, **2010**, 1-4.
16. Dr. Kimberly Cipolla, Dr. William Keith, Dr. Alia Foley, SPIV Measurements of Axisymmetric Turbulent Boundary Layers, *Oceans*, **2010**, 1-7.
17. Z. Liancun, Z. Xinxin, Shear Force Distribution and Heat Transfer in Laminar Boundary Layer Flows for Power Law Fluid, *Tsinghua Science and Technology*, **2002**, 7, 182-186.
18. W. Balzer, A. Gross, H.F. Fasel, Control of Boundary-Layer Separation for Lifting Surfaces, *DoD High Performance Computing Modernization Program Users Group Conference*, **2009**, 37-45.
19. N.A. Kudryashov, M.B. Kochanov, General and approximate solutions of the boundary layer equation for radial flow of incompressible liquid, *International Journal of Non-Linear Mechanics*, **2015**, 248-253.
20. S. Talpos, M. Apostol, Displaced logarithmic profile of the velocity distribution in the boundary layer of a turbulent flow over an unbounded flat surface, *Physics Letters A*, **2015**, 379, 3102-3107.
21. C.J. Doolan, D.J. Moreau, Flow-induced noise generated by sub-boundary layer steps, *Experimental Thermal and Fluid Science*, **2016**, 72, 47-58.
22. G.V. Veres, O.R. Tutty, E. Rogers, P.A. Nelson, Parallel global optimisation based control of boundary layer transition, **2003,7th European Control Conference, Cambridge, UK**, 3225-3230.
23. B.N. Rajani, A. Kandasamy, S. Majumdar, Numerical simulation of laminar flow past a circular cylinder, *Applied Mathematical Modelling*, **2009**, 33, 1228-1247.
24. D. Arnal, G. Casalis, Laminar-turbulent transition prediction in three-dimensional flows, *Progress in Aerospace Sciences*, **2000**, 36, 173-191.
25. G. Xia, D. Ma, Y. Zhai, Y. Li, R. Liu, M. Du, Experimental and numerical study of fluid flow and heat transfer characteristics in microchannel heat sink with complex structure, *Energy Conversion and Management*, **2015**, 105, 848-857.
26. C. Norberg, Flow around a circular cylinder: Aspects of Fluctuating Lift, *Journal of Fluids and Structures*, **2001**, 15, 459-469.
27. S. Singha, K.P. Sinhamahapatra, Flow past a circular cylinder between parallel walls at low Reynolds numbers, *Ocean Engineering*, **2010**, 37, 757-769.
28. C. Pozrikidis, Shear flow over cylindrical rods attached to a substrate, *Journal of Fluids and Structures*, **2010**, 26, 393-405.
29. R. Duvigneau, M. Visonneau, Hydrodynamic design using a derivative-free method, *Structural Multidisciplinary Optimization*, **2004**, 28, 195-205.
30. Comsol Multiphysics User Manual, COMSOL Multiphysics Ver 5.0, 2014.
31. Z. Dai, Z. Zheng, D.F. Fletcher, B.S. Haynes, Experimental study of transient behaviour of laminar flow in zigzag semi-circular microchannels, *Experimental Thermal and Fluid Science*, **2015**, 68, 644-651.
32. E. Lund, H. Møller, L.A. Jakobsen, Shape design optimisation of stationary fluid-structure interaction problems with large displacements and turbulence, *Structural Multidisciplinary Optimization*, **2003**, 25, 383-392.